Title
Single-cell mobility shift electrophoresis reports protein localization to the cell membrane

Journal
Analyst, 144(3)

ISSN
0003-2654

Authors
Sinkala, Elly
Rosàs-Canyelles, Elisabet
Herr, Amy E

Publication Date
2019-01-28

DOI
10.1039/c8an01441h

Peer reviewed

HHS Public Access

Author manuscript

Analyst. Author manuscript; available in PMC 2020 January 28.

Published in final edited form as:

Analyst. 2019 January 28; 144(3): 972–979. doi:10.1039/c8an01441h.

Single-cell mobility shift electrophoresis reports protein localization to the cell membrane

Elly Sinkala[a,†], **Elisabet Rosàs-Canyelles**[a,b,†], and **Amy E. Herr**[a,b]

[a]Departement of Bioengineering, University of California, Berkeley, 94720 Berkeley USA

[b]The Univeristy of California, Berkeley and University of California, San Francisco Graduate Program in Bioengineering, 94270 Berkeley, USA

Abstract

While profiling of cell surface receptors grants valuable insight on cell phenotype, surface receptors alone cannot fully describe activated downstream signaling pathways, detect internalized receptor activity, or indicate constitutively active signaling in subcellular compartments. To measure surface-bound and intracellular targets in the same cell, we introduce a tandem single-cell assay that combines immunofluorescence of surface-bound epithelial cellular adhesion molecule (EpCAM) with subsequent protein polyacrylamide gel electrophoresis (PAGE) of unfixed MCF7 breast cancer cells. After surface staining and cell lysis, surface EpCAM is analyzed by single-cell PAGE, concurrent with immunoprobing of intracellular targets. Consequently, the single-cell electrophoresis step reports localization of both surface and intracellular targets. Unbound intracellular EpCAM is readily resolved from surface EpCAM immunocomplex owing to a ~30% mobility shift. Flow cytometry and immunofluorescence are in concordance with single-cell PAGE. Lastly, we challenged the stability of the EpCAM immunocomplexes by varying ionic and non-ionic component concentrations in the lysis buffer, the lysis time, and electrophoresis duration. As expected, the harsher conditions proved most disruptive to the immunocomplexes. The compatibility of live-cell immunostaining with single-cell PAGE eliminates the need to perform single-cell imaging by condensing read-out of both surface-bound proteins (as low mobility immune complexes) and intracellular targets to a single immunoblot, thus linking cell type and state.

Graphical Abstract

†E.S. and E.R.C. contributed equally to this work. E.S., E.R.C., and A.E.H. devised experiments. E.S. and E.R.C. conducted experiments and data analysis and constructed figures. All authors wrote the manuscript.

Conflicts of interest

There are no conflicts to declare.

Electronic Supplementary Information (ESI) available: [details of any supplementary information available should be included here]. See doi: 10.1039/c8an01441h

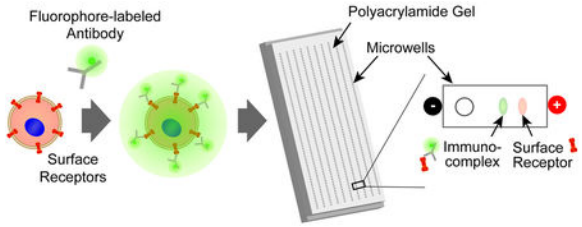

Introduction,

Cell surface receptors are responsible for responding to local or distal soluble factors. Surface receptors bind ligands on the surface of other cells to mediate cell-to-cell interactions, as well as sense and transduce physical cues from the microenvironment(1,2). Measuring the expression of surface receptors on a cell is useful for identifying cell types and examining phenotypes(3-6). However, measuring the expression of surface-bound receptors alone is not enough to fully describe cellular state(7). First, the *localization* of surface receptors more accurately depicts the phenotype of a cell than the total expression. For instance, measuring receptors not bound to the cell surface becomes crucial in cases where constitutively active surface receptors can signal from intercellular compartments(8) with the expression of constitutively active isoforms that lack the extracellular domain, or when receptors are not bound to the membrane(9). Second, when establishing surface receptor-mediated signaling, measuring the abundance and activation of proteins in the downstream signaling pathways is as important as measuring surface receptors. This becomes extremely important in cases where a given receptor activates multiple signaling pathways, so measuring abundance of the surface receptor when only on the surface cannot reveal the specific proteins and genes involved(10,11). Thus, in order to fully characterize cellular phenotype and state, we require tools to measure (i) the abundance of surface markers on the surface of cells in conjunction with (ii) internalized surface receptors and (iii) intracellular proteins in the downstream signaling pathways.

Gold standard tools that measure surface receptors along with intracellular targets (i.e., flow cytometry and immunofluorescence) employ antibodies probes for target specificity(12-14). However, antibody probes present confounding limitations including cross-reactivity with off-target proteins and an inability to detect protein isoforms (when isoform-specific antibodies are not available)(15,16). Furthermore, cells must often be chemically fixed and permeabilized to measure intracellular targets. Surface-localized versus internalized receptors can become indistinguishable, and fixation artifacts can emerge (e.g., epitope masking, changes in morphology and protein localization due to formation of diffusional gradients as fixation occurs(17-19)).

To overcome the lack of immunoassay specificity, a protein separation is prepended to the immunoassay (e.g., immunoblotting). Separating proteins by electrophoresis first resolves target protein signal from off-target binding events, as well as facilitates detection of mass- or charge-differing protein isoforms, even when an isoform-specific antibody is lacking. If the electrophoresis step is protein sizing, the immunoblot is called a western blot. Other forms exist. Conventional slab-gel western blotting requires ~10^3 cells for analysis, thus

precluding the single-cell resolution achievable with flow cytometry and IF. Recently introduced single-cell immunoblotting, employing single-cell PAGE(20-22), uses microfluidic design and photo-activatable protein capture chemistry for precision control and analysis of individual cells. In combination, the approaches act to minimize diffusional losses during the electrophoresis and blotting stages. Furthermore, the covalent immobilization of PAGE-resolved proteins to the hydrogel scaffold facilitates multiplexing of 10+ targets per single cell through rounds of chemical stripping and reprobing. Nonetheless, single-cell immunoblotting uses whole-cell lysis before the single-cell PAGE step, thus obscuring the location of surface versus internal proteins.

Consequently, we introduce a microfluidic immunoblot that reports on both surface-bound cellular receptors and intracellular proteins, using a single-cell immunoblot readout. We focus on epithelial cellular adhesion molecule (EpCAM), a surface receptor involved in cell proliferation in healthy differentiation and growth as well as in the progression of diseases such as cancer (23,24). EpCAM is a cell surface glycoprotein that, along with other cellular adhesion molecules, maintains the epithelial barrier function by forming tight junctions between the apical and basolaterial domains of epithelial cells(24). Interestingly, mutations in the EpCAM gene can prevent localization of the receptor to the cell membrane (23-25). In order to investigate EpCAM localization, we first isolate live, individual MCF7 cells in microwells and immunostain each with fluorescently tagged antibody against EpCAM. In-microwell chemical cell lysis and subsequent PAGE resolves the surface-bound EpCAM from intracellular proteins (in the polyacrylamide gel surrounding each microwell). We observe stable electromigration of surface EpCAM immunocomplexes, a significant decrease in electrophoretic mobility of the large surface EpCAM immunocomplex with respect to the free intracellular EpCAM (mobility shift), and that co-migration of the surface EpCAM immunocomplex does not interfere with the electromigration of other lysate proteins. To challenge the stability of the surface EpCAM immunocomplex during single-cell PAGE, we varied lysis and electrophoresis conditions, thus determining that primary importance of the lysis buffer detergent concentrations. Prepending surface receptor immunostaining with single-cell PAGE provides a new tool with which to understand how under- or over-expression of surface receptor proteins controls the complex regulatory systems in single cells.

Results and Discussion

Surface receptor complexes are stably intact during single-cell PAGE

Given the importance of correlating surface receptor localization to activation of intracellular signaling, we sought to understand if surface EpCAM immunocomplexes are detectable using single-cell immunoblotting. Single-cell immunoblotting can analyze 100s to 1000s of individual cells in ~4 hours. The device consists of a 40 μm thick PA gel affixed to a standard microscope slide. The thin gel layer is stippled with 30 μm diameter microwells (Fig. 1, A). To investigate migration of immunocomplexes, cells are first immuno-stained with fluorophore-labeled antibodies to a surface receptor target (Fig. 1, B). Stained cells are then sedimented into the microwells (Fig. 1, C). Microwell dimensions are designed to maximize single-cell-per-microwell occupancy, where microwell diameter approximates the

average cell diameter and the diameter-to-height ratio is kept at 3:4 to prevent multiple cells from stacking into the microwells(22). A dual-functionality cell lysis and electrophoresis buffer is used to lyse cells, solubilize proteins, and support electrophoresis. After cell lysis, an electric field is applied to (i) electrophoretically inject proteins into the PA gel and (ii) separate proteins by single-cell PAGE. After protein separation, the migrated proteins are covalently bound to the PA gel by UV-mediated activation of benzophenone-methacrylamide monomers crosslinked into the PA gel. For protein detection, PA gels are immunoprobed with primary and fluorescently tagged secondary antibodies.

We assessed the dual capacity of the surface immunocomplexes to (i) electromigrate into the molecular sieving gel (immunocomplex is ~290 kDa) and (ii) remain associated, even after single-cell lysis and PAGE, by assaying EpCAM-stained MCF7 cells. After isolating single, live MCF7 cells in microwells, we stained the cells with an AlexaFluor 488-labeled antibody against EpCAM (termed here anti-EpCAM*) (Fig. 1, D). To support protein PAGE for a wide molecular mass range, we selected a moderate pore-size (7–8%T) PA gel and 3–4x longer separation distance than previously employed (here 1.5 – 2 mm)[17]. We performed single-cell PAGE and UV-activated protein immobilization. Upon imaging the gel, we observed fluorescent bands in the separation lane abutting each cell-laden microwell, indicating successful electroinjection and electromigration of the fluorescently-labeled antibody into the PA gel (Fig. 1, D).

To investigate the mobility shift between the surface EpCAM immunocomplexes and free EpCAM, we simultaneously assayed unstained MCF7 cells, a population of surface EpCAM immunostained cells, and cells stained with an isotype-matched antibody control (also labeled with AlexaFluor488). To control for device-to-device variation in electrophoretic migration, we also simultaneously assayed load control protein, GAPDH. We did not observe significant differences in the electromigration of GAPDH across the three experimental groups (Fig. S1, Kruskall-Wallis statistic = 3.251, p value = 0.1968, 3 groups tested, N = 37 total). We first examined single-cell PAGE of the isotype-matched control and the unstained MCF7 experimental groups for immunocomplex bands. As expected, neither group showed detectable fluorescence signal for the AlexaFluor488 immunocomplex (Fig. 2, A). Upon immunoprobing for EpCAM after single-cell PAGE, both experimental groups reported detectable signal for free EpCAM (Fig. 2, A).

For the EpCAM immunostained cells, on the other hand, we detected fluorescent immunocomplex bands at 0.209 ± 0.023 mm down the separation axis (mean ± SD, N = 37, Fig. 2, A, green band). Upon in-gel immunoprobing using the same anti-EpCAM* as the primary probe, we detected a lower molecular mass protein band at 0.272 ± 0.040 mm (Fig. 2, A, blue band), which is a statistically significant difference in migration distance (Mann Whitney U test, p value < 0.0001, N = 37, Fig. 2, B). We attribute the high molecular mass peak to the surface EpCAM immunocomplex (from surface staining) and posit that the lower molecular mass peak corresponds to the intercellular fraction of EpCAM (assuming excess anti-EpCAM during surface staining). Intracellular EpCAM is not accessible to immunoprobe binding using surface staining. Consequently, the method reported here reports the localization of receptors to the cell surface or to the intracellular compartment using a mobility shift in the bound versus unbound EpCAM target.

Stability of surface receptor complexes is sensitive to cell lysis and electrophoresis conditions

We next examined the sensitivity of the surface EpCAM immunocomplex stability on the lysis and electrophoresis conditions used for single-cell PAGE. In single-cell PAGE of surface-stained MCF7 cells, we applied different lysis buffer compositions, lysis times ($t_{\mathbf{lysis}}$), and electrophoresis times ($t_{\mathbf{EP}}$) and compared (i) surface EpCAM immunocomplex signal (area-under-the-curve, or AUC) and (ii) EpCAM immunocomplex protein peak electromigration distance.

We first investigated the effects of lysis buffer composition on disruption of surface EpCAM immunocomplex. The dual function cell lysis and electrophoresis buffer comprises both non-ionic and anionic detergents. Detergents commonly employed for cell lysis and protein solubilization are Triton X-100, sodium deoxycholate (Na-DOC), and sodium dodecyl sulfate (SDS). The non-ionic detergent Triton X-100 lyses cells by disrupting the phospholipid bilayer of the cellular membrane, while the ionic detergents (SDS and Na-DOC) denature cellular proteins by hydrophobic interaction with the hydrophobic protein residues, generally buried in the structure of folded proteins, to form detergent-protein complexes(26). While Triton X-100 has been shown to have mild effects on antibody-antigen interaction (and no concentration-dependent effects seen for a range of 0.1 to 5%,), Na-DOC and SDS show concentration-dependent effects on disruption of antibody-antigen complexes(26). Thus, a tradeoff exists between (i) the need to incorporate Na-DOC and SDS for complete protein solubilization in order to resolve proteins by PAGE and (ii) the disruptive effects of Na-DOC and SDS on antibody-antigen complexes.

To assess EpCAM immunocomplex stability, we formulated three lysis buffers spanning a range of stringencies: (1) mild with 0.5X Tris/Glycine/0.5% SDS/0.1% Triton X-100/0.25% Na-DOC, (2) moderate with 0.5X Tris/Glycine/1.0% SDS/0.1% Triton X-100/0.25% Na-DOC, and (3) harsh with 0.5X Tris/Glycine/1.0% SDS/1.0% Triton X-100/0.5% Na-DOC with conductivities of 1.21, 1.49 and 1.99 mS/cm, respectively. For each lysis buffer composition, we applied the single-cell PAGE assay to MCF7 cells stained with anti-EPCAM* and assessed surface EpCAM immunocomplex levels using fluorescence imaging.

We first scrutinized the effects of buffer composition on electrophoretic migration distance of the surface EpCAM immunocomplex. Between the mild to moderate lysis buffer conditions, we observed a significant increase in the migration distance of the surface EpCAM immunocomplex peak (130 ± 24.46 μm and 146.5 ± 8.06 μm, Mann Whitney U test p-value < 0.0001 for N = 387 and 670, respectively; Fig. 3, A). Between the moderate to harsh lysis buffer conditions we likewise observed a significant increase in migration distance (146.5 ± 8.06 μm and 215 ± 19.56 μm, Mann Whitney U test p-value < 0.0001 for N = 670 and 59, respectively; Fig. 3, A). We attribute increased migration distance with each more stringent lysis buffer composition to the increased conductivity of lysis buffers (arising from higher detergent concentrations).

For each lysis buffer composition, we next measured the AUC of the surface EpCAM immunocomplex peak along the single-cell PAGE separation axis. Assuming no differential interference with fluorescence from the AlexaFluor 488, we assume that the AUC of each

peak is a proxy for the total mass of anti-EpCAM* present. Given a single peak, we further assume that the peak also reports the amount of surface EpCAM immunocomplex present from each surface stained cell. We observed increased surface EpCAM immunocomplex AUC with increased lysis buffer stringency from mild to moderate lysis buffer conditions (AUC, Mann Whitney U test, p-value < 0.001 for N = 387 and 670, respectively; Fig. 3, A). The observation suggests increased efficacy in electrophoretic injection of surface EpCAM immunocomplex from the microwell into the PA gel. Intriguingly, increasing the lysis buffer stringency from moderate to harsh conditions resulted in a significant reduction in surface EpCAM immunocomplex AUC (Mann Whitney U test, p-value < 0.0001, for N = 59 and 670, respectively; Fig. 3, A). This reduction in surface EpCAM immunocomplex AUC suggests that the concentration of detergents in the harsh lysis buffer may disrupt the immunocomplex binding.

Next, we considered design of the cell lysis step and a trade-off that arises between: (i) the lysis duration required for effective solubilization of cellular proteins and (ii) time-dependent protein losses occurring during the lysis step (stemming from diffusion of lysate out of the open microwell). To investigate this trade-off, we varied the $t_{\mathbf{lysis}}$ for MCF7 cells (10, 20, and 30 s) with the mild lysis buffer, while maintaining a constant $t_{\mathbf{EP}}$ = 25 s. The migration distance of the surface EpCAM immunocomplex peak was significantly different for all conditions. Given that t_{lysis} = 20 s shows the longest average migration distance (Mann Whitney U test p-values all < 0.0001, Fig. 3, B), we hypothesize that (i) at lower lysis times (i.e. t_{lysis} = 10 s) insufficient lysis before the start of EP causes continuous injection, skewing the shape of the band and thus decreasing the average migration distance and (ii) at t_{lysis} = 30 s, higher diffusional losses cause the leading band edge to fall under the limit of detection. Additionally, we found a significant increase in surface EpCAM immunocomplex AUC from the $t_{\mathbf{lysis}}$ =10 s to the $t_{\mathbf{lysis}}$ = 20 s condition, followed by a significant reduction in EpCAM immunocomplex AUC from the $t_{\mathbf{lysis}}$ = 20 s to the $t_{\mathbf{lysis}}$ = 30 s condition (Mann Whitney U test p-values all < 0.0001, Fig. 3, B). Thus, the surface EpCAM immunocomplex AUC is sensitive to a balance between adequate solubilization of proteins (needed for effective injection of protein into the gel) and increased diffusive lysate losses out of the microwell at longer $t_{\mathbf{lysis}}$. The reduction in AUC at $t_{\mathbf{lysis}}$ = 30s supports this assertion. Hence, $t_{\mathbf{lysis}}$ = 20s was selected to balance this trade-off.

Finally, we investigated the impact of the electrophoresis duration on the stability of the surface EpCAM immunocomplex peak. Surface stained MCF7 cells housed in microwells were lysed at $t_{\mathbf{lysis}}$ = 20 s with the mild lysis buffer and assayed at three $t_{\mathbf{EP}}$ (15, 25, and 35s). We observed a significant increase in the AUC of the surface EpCAM immunocomplex peak for the $t_{\mathbf{EP}}$ = 25 s and the $t_{\mathbf{EP}}$ = 35 s conditions, as compared to the short $t_{\mathbf{EP}}$ = 15 s (Mann Whitney U test, p values < 0.0001 for 15 s versus 25 s and 15 s versus 35 s, with N = 539, 567 and 854 cells for 15, 25 and 35 s respectively; Fig. 3, C). Interestingly, we found that increasing the $t_{\mathbf{EP}}$ from 25 to 35 s caused a decrease in the AUC of the surface EpCAM immunocomplex peak (Mann Whitney U test, p value < 0.0001, for N = 567 and 854, respectively; Fig. 3, C). Similar to the $t_{\mathbf{lysis}}$ = 10 s observation, we attribute a lower AUC for the surface EpCAM immunocomplex peak at $t_{\mathbf{EP}}$ = 15 s to minimal injection of the large complex into the gel. We further hypothesize that a temperature rise may occur under these conditions, causing more diffusional losses out of the open microwell (and top of the PA gel

layer). A temperature rise – and associated increase in diffusion coefficients of the protein targets – would be caused by Joule heating, the resistive heating that arises from electrical current passing through an electrolyte(27). We would expect to observe the largest temperature increases at the longest t_{EP} (i.e., 35 s). Increased diffusional losses reduce the AUC for the surface EpCAM immunocomplex.

Under the conditions described here, surface EpCAM immunocomplex stability is most sensitive to the high ionic detergent concentrations, perhaps through enhanced k_{off} of the anti-EpCAM* from the surface EpCAM immunocomplex. While the electrophoresis conditions ($t_{\mathbf{lysis}}$, $t_{\mathbf{EP}}$) do play a role in assay performance, our results suggest diffusive losses and inadequate sample injection are more important than immunocomplex stability *per se*. Furthermore, application of this technology to other targets will require optimizing cell lysis and EP conditions. For instance, a protein target of higher molecular mass might require longer EP times in order to achieve injection into the PA gel, while a target of lower molecular mass might require shorter EP times to prevent excessive diffusional losses during electromigration.

Validating single-cell PAGE with conventional flow cytometry and IF

We next sought to examine whether the fluorescence intensity distributions of anti-EpCAM* stained cells obtained by single-cell PAGE is corroborated by gold standard flow cytometry and IF. In a first line of inquiry, we examined whether flow cytometry and single-cell PAGE report similar fluorescence intensity distribution over a range of anti-EpCAM* concentrations. We created MCF7 cell suspensions and stained each with a different concentration of anti-EpCAM* (0.1, 1.0, 3.0 and 5.0 μg/mL). The cell suspensions from each staining condition were split into 2 vials for analysis by either flow cytometry or single-cell PAGE (moderate lysis buffer, $t_{\mathbf{lysis}}$ = 20 s, $t_{\mathbf{EP}}$ = 25 s). Fluorescence intensity distributions for flow cytometry and single-cell PAGE showed similar trends, where stained cells show high overlap when stained at 1, 3 and 5 g/uL (flow cytometry: 85.8% for 1 mg/mL versus 3 mg/mL, 81.2% for 1 mg/mL versus 5 mg/mL and 87.8% for 3 mg/mL versus 5 mg/mL; single-cell PAGE: 61.7% for 1 mg/mL versus 3 mg/mL, 67.7 % for 1 mg/mL versus 5 mg/mL and 67.4 mg/mL for 3 mg/mL versus 5 mg/mL; Fig. 4, A and B).

At the lowest concentration (0.1 μg/mL) the fluorescence distributions of the cells showed low overlap between single-cell PAGE and flow cytometry (overlap with 0.1 μg/mL for flow cytometry: 6.62% for 1 μg/mL, 5.76% for 3 μg/mL and 7.44% for 5 μg/mL; overlap with 0.1 μg/mL for single-cell PAGE: 26.4% with 1 μg/mL, 29.9% with 3 μg/mL and 32.4 with 5 μg/mL, Fig. 4, A and B). Flow cytometry validated that the 0.1 μg/mL concentration condition shows higher overlap with the negative control (69.6% for negative control versus 0.1 mg/mL, Fig. 4, A and B) than do the higher concentration conditions We surmise that surface receptors are not saturated at the 0.1 g/mL anti-EpCAM* staining condition, which is observable through both flow cytometry and single-cell PAGE.

In a second line of inquiry, we examined concordance between IF and single-cell PAGE of surface-stained cells. MCF7 cells were stained with FITC-anti-EpCAM at 3 mg/mL to saturate EpCAM surface receptors. Cells were then settled into microwells of a single-cell PAGE device and imaged by fluorescence microscopy for surface-bound FITC-anti-

EpCAM. Single-cell PAGE (moderate lysis buffer, $t_{\mathbf{lysis}}$ = 20 s $t_{\mathbf{EP}}$ = 25 s) and UV-activated immunoblotting were performed on the stained cells. The anti-EpCAM immunoblots showed a significant positive linear correlation between the IF-based surface anti-EpCAM signal and single-cell PAGE anti-EpCAM signal (Pearson correlation, $\rho = 0.694$, p value < 0.00001, N = 148 microwells containing single cells; Fig. 4, C). The results suggest that single-cell PAGE is an accurate proxy for surface stained EpCAM receptors even after cell lysis, electrophoresis, and photocapture.

Experimental

Antibodies.

The primary antibodies in the surface staining characterization experiments include EpCAM-FITC (mouse, mAb, SAB4700424, Sigma), IgG-FITC (mouse, mAB, SA1–12320, Pierce), EpCAM-AlexaFluor 488 (mouse, mAb, 53–8326-42, Ebioscience), primary protein antibodies to GAPDH (goat pAb; SAB2500450, Sigma), β-Tubulin (rabbit pAb; ab6046, Abcam). Secondary antibodies to goat IgG prelabeled with Alexa Fluor 488 and 555 (A11055 and A21432) were purchased from Invitrogen.

Chemicals.

30%T, 2.7%C acrylamide/bis-acrylamide (37.5:1) (A3699), ammonium persulfate (APS, A3678), and tetramethylethylenediamine (TEMED, T9281), bovine serum albumin (BSA, A7638), fetal bovine serum (FBS, F2442) were purchased from Sigma-Aldrich. Triton X-100 (BP-151), phosphate buffered saline (PBS, 10010023), RPMI 1640 medium 11875, penicillin-streptomycin 15070063 were purchased from ThermoFisher Scientific. Premixed 10× Tris/glycine/SDS electrophoresis buffer (25 mM Tris, pH 8.3; 192 mM glycine; 0.1% SDS) was purchased from Bio-Rad. Deionized water (18.2 MΩ) was obtained using an Ultrapure water system from Millipore. *N*-[3-[(3-Benzoylphenyl)formamido]propyl] methacrylamide (BPMAC) was custom synthesized by PharmAgra Laboratories(20,21). Conductivity of lysis buffers was measured with a Twin Condo conductivity meter (B-173, Horiba).

SU8 and polyacrylamide (PA) gel fabrication.

SU8 fabrication to generate the master and PA gel fabrication were performed as described previously(21). The cell line experiments used a 7%T PA gel, and the microwell diameter and depth of 30 μm and 40 μm respectively. All PA gels on the single-cell PAGE slides were chemically polymerized with 0.08% APS and 0.08% TEMED.

Cell lines and surface staining.

MCF7 cells were obtained from the American Type Culture Collection (ATCC) and authenticated (Promega). The MCF7 cell line was maintained in RPMI 1640 supplemented with 1% penicillin/streptomycin, 0.01mg/mL insulin (Invitrogen) and 10% FBS. Cells were kept in a 37°C incubator at 5% CO_2. For surface staining, cells were harvested with 0.25% Trypsin EDTA and resuspended in 4°C 3% BSA in PBS at a concentration of ~10^7 cells/mL. In a 1.5 mL Eppendorf tube, 4°C PBS+3% BSA, 5 μL of cell suspension, and the staining solution (anti-EpCAM Alexa 488 or IgG control) were added to a total volume of 500 μL. A

control tube included only the PBS+3% BSA and cell suspension. Cells were stained for 30 min in the dark on ice. In order to remove excess anti-EpCAM, tubes were centrifuged at 1000 RCF and the supernatant was carefully removed. Cells were then washed twice by resuspending cells with 400 μL of fresh 4°C PBS, pelleting cells at 1000 RCF, aspirating and discarding supernatant. Prior to single-cell PAGE, cells were resuspended to a concentration of ~10^6 cells/mL. For the titration experiments, we tested a range of antibody concentration (0.1, 1.0, 3.0 and 5.0 μg/mL) and 3.0 μg/mL was used for the remaining experiments.

Single-cell PAGE.

Cells were pipetted over the PA gel and allowed to settled by gravity into the microwells patterned in the PA gel. Lysis buffer heated in a water bath to 50°C was poured over the PA gel in order to lyse the cells in the microwells. An electric field (E = 40 V/cm) was applied to inject and separate proteins in the PA gel abutting the microwell. After separation, proteins were immobilized to the gel matrix via UV activation (Lightningcure LC5, Hamamatsu) of benzophenone methacrylamide cross-linked into the PA gel. Immobilized proteins were probed in-gel by diffusing fluorescently labeled antibody probes into the PA. A fluorescence microarray scanner (Genepix 4300A, Molecular Devices) equipped with 4-laser lines (λ = 488, 532, 594, 635) acquired fluorescence readout. Subsequent rounds of antibody stripping were performed for multiplexed protein analysis, as detailed previously(21).

Single-cell PAGE and flow cytometry validation.

MCF7 cells were stained with 0.1, 1.0, 3.0 and 5.0 μg/mL of the antibody solution, as previously described, and placed into four separate centrifuge tubes. A negative control was prepared with unstained cells. For each tube, a 200 μL of the cell suspension was placed into a 96-well plate for flow analysis (Guava EasyCyte 6HT). The remaining cells were processed with by single-cell PAGE. The negative control with unstained cells was used for thresholding, and a total of 5000 events were counted per antibody concentration.

Immunoblot signal quantification and statistical analysis.

The data sets reported here are available from the corresponding author on reasonable request. Quantification of fluorescence signal from immunoblots used in-house scripts written in MATLAB (R2014b) as previously described(28). Gaussian curves were fit to fluorescence intensity profiles in MATLAB (R2014b, Curve Fitting Toolbox) in order to obtain the mean, μ (used to describe the protein migration distance) and the variance σ^2 (used to calculate peak width as 4*σ). Area-under-the-curve (AUC) analysis of the intensity profiles was performed to quantify immunoblot signal. Statistical tests were performed with GraphPad Prism 7.0b.

Conclusions

Surface staining of intact cells plays a critical role in identifying specific cell subpopulations. We introduce a single-cell mobility shift assay that reports surface receptor levels in unfixed mammalian cells. We surface stain cells with fluorescently labeled antibody after isolating individual cells in microwells. After isolation, we perform chemical cell lysis

and single-cell protein PAGE, measuring a mobility shift between surface EpCAM immunocomplex and intracellular EpCAM. The mobility difference stems from the fact that EpCAM that is localized to the cell surface is accessible to anti-EpCAM* surface stain while EpCAM localized to the intracellular compartments is not and, thus, does not form an immunocomplex with the anti-EpCAM* stain. We detect the unbound, intracellular EpCAM by immunoprobing of single-cell PAGE.

During single-cell PAGE, we observe no notable interference between the large immunocomplex and intracellular proteins (i.e., no detectable impact on GAPDH migration distance for surface-stained and unstained cells). Gold standard flow cytometry reports a similar anti-EpCAM* fluorescence distribution to that reported by single-cell PAGE for a range of anti-EpCAM concentrations (0.1 – 5 μg/mL). The results support the assertion that single-cell PAGE accurately measures surface-bound receptors through formation and mobility shift of immunocomplexes.

We were curious about the stability of the surface EpCAM immunocomplexes under cell lysis and electrophoresis conditions, and scrutinized the stability for a range of cell lysis buffers, lysis times, and electrophoresis times. Our analysis suggestions that surface EpCAM immunocomplex stability is most sensitive to the detergent concentration of lysis buffer, for the system and conditions described here. The integration of surface receptor staining of live cells with single-cell PAGE provides a single mobility shift readout representative of protein target localization and cell phenotype.

Supplementary Material

Refer to Web version on PubMed Central for supplementary material.

Acknowledgements

The authors acknowledge members and alumni of the Herr Lab for helpful discussions. Partial infrastructure support was provided by the QB3 Biomolecular Nanofabrication Center. This research was performed under a National Institutes of Health Training Grant awarded to the UCB/USCF Graduate Program in Bioengineering (5T32GM008155–29 to E.R.C.), a California Institute for Regenerative Medicine Predoctoral Fellowship (E.R.C.), an Obra Social “la Caixa” Fellowship (E.R.C.), a University of California, Berkeley Siebel Scholarship (E.R.C.), a National Science Foundation CAREER Award (CBET-1056035 to A.E.H.), National Institutes of Health grants (1R01CA203018 to A.E.H).

Notes and references

1. Uings IJ, Farrow SN. Cell receptors and cell signalling. J Clin Pathol Mol Pathol. 2000;53:295–9.
2. Schwartz MA, DeSimone DW. Cell adhesion receptors in mechanotransduction. Curr Opin Cell Biol. 2008;20(5):551–6. [PubMed: 18583124]
3. Brockhoff G, Hofstaedter F, Knuechel R. Flow Cytometric Detection and Quantitation of the Epidermal Growth-Factor Receptor in Comparison To Scatchard Analysis in Human Bladder-Carcinoma Cell-Lines. Cytometry. 1994;17:75–83. [PubMed: 8001460]
4. Fenderson BA, Miguel MP De, Pyle AD, Donovan PJ. Antibodies to Stage-Specific Embryonic Antigens. Methods Mol Biol. 325:207–24. [PubMed: 16761728]
5. Zhang S, Balch C, Chan MW, Lai H-C, Matei D, Schilder JM, et al. Identification and Characterization of Ovarian Cancer-Initiating Cells from Primary Human Tumors. Cancer Res. 2008;68(11):4311–20. [PubMed: 18519691]

6. Cheang MCU, Chia SK, Voduc D, Gao D, Leung S, Snider J, et al. Ki67 index, HER2 status, and prognosis of patients with luminal B breast cancer. J Natl Cancer Inst. 2009;101(10):736–50. [PubMed: 19436038]
7. Lustberg MB, Balasubramanian P, Miller B, Garcia-Villa A, Deighan C, Wu Y, et al. Heterogeneous atypical cell populations are present in blood of metastatic breast cancer patients. Breast Cancer Res. 2014;16(2).
8. Prasad BM. Methods to detect cell surface expression and constitutive activity of GPR6. Methods Enzym. 2010;484:179–95.
9. Ward TM, Iorns E, Liu X, Hoe N, Kim P, Singh S, et al. Truncated p110 ERBB2 induces mammary epithelial cell migration, invasion and orthotopic xenograft formation, and is associated with loss of phosphorylated STAT5. Oncogene. 2013;32(19):2463–74. [PubMed: 22751112]
10. Mitsuhashi M, Payan DG. Multiple signaling pathways of histamine H2 receptors. J Biol Chem. 1989;264(31):18356–62. [PubMed: 2553705]
11. Wang D, Liu C, Wang J, Jia Y, Hu X, Jiang H, et al. Protein C receptor stimulates multiple signaling pathways in breast cancer cells. J Biol Chem. 2018;293(4):1413–24. [PubMed: 29217770]
12. Perfetto SP, Chattopadhyay PK, Roederer M. Seventeen-colour flow cytometry: Unravelling the immune system. Nat Rev Immunol. 2004;4(8):648–55. [PubMed: 15286731]
13. Bendall SC, Nolan GP, Roederer M, Chattopadhyay PK. NIH Public Access. Trends Immunol. 2012;33(7):323–32. [PubMed: 22476049]
14. Cram LS. Flow cytometry, an overview L. Methods Cell Sci. 2002;24:1–9. [PubMed: 12815284]
15. Bradbury A, Plückthun A. Reproducibility: Standardize antibodies used in research. Nature. 2015;518(7537):27–9. [PubMed: 25652980]
16. Berglund L, Björling E, Oksvold P, Fagerberg L, Asplund A, Al-Khalili Szigyarto C, et al. A Genecentric Human Protein Atlas for Expression Profiles Based on Antibodies. Mol Cell Proteomics. 2008;7(10):2019–27. [PubMed: 18669619]
17. Schnell U, Dijk F, Sjollema KA, Giepmans BNG. Immunolabeling artifacts and the need for live-cell imaging. Nat Methods. 2012;9(2):152–8. [PubMed: 22290187]
18. Teves SS, An L, Hansen AS, Xie L, Darzacq X, Tjian R. A dynamic mode of mitotic bookmarking by transcription factors. Elife. 2016;5(e22280):1–24.
19. Chatterjee S Artefacts in histopathology. J Oral Maxillofac Pathol. 2014;18(Suppl 1):S111–6. [PubMed: 25364159]
20. Kang CC, Lin JMG, Xu Z, Kumar S, Herr AE. Single-cell western blotting after whole-cell imaging to assess cancer chemotherapeutic response. Anal Chem. 2014;86(20):10429–36. [PubMed: 25226230]
21. Hughes AJ, Spelke DP, Xu Z, Kang C-C, Schaffer D V, Herr AE. Single-cell western blotting. Nat Methods. 2014;11(7):749–55. [PubMed: 24880876]
22. Kang C-C, Yamauchi KA, Vlassakis J, Sinkala E, Duncombe TA, Herr AE. Single cell–resolution western blotting. Nat Protoc. 2016;11(8):1508–30. [PubMed: 27466711]
23. Munz M, Baeuerle PA, Gires O. The emerging role of EpCAM in cancer and stem cell signaling. Cancer Res. 2009;69(14):5627–9. [PubMed: 19584271]
24. Schnell U, Cirulli V, Giepmans BNG. EpCAM: Structure and function in health and disease. Biochim Biophys Acta. 2013;1828:1989–2001. [PubMed: 23618806]
25. Baeuerle PA, Gires O. EpCAM (CD326) finding its role in cancer. Br J Cancer. 2007;96(3):417–23. [PubMed: 17211480]
26. Qualtiere LF, Anderson AG, Meyers P. Effects of Ionic and Nonionic Detergents on Antigen-Antibody Reactions. J Immunol. 1997;119:1645–51.
27. Evenhuis CJ, Haddad PR. Joule heating effects and the experimental determination of temperature during CE. Electrophoresis. 2009;30(5):897–909. [PubMed: 19197907]
28. Sinkala E, Sollier-Christen E, Renier C, Rosàs-Canyelles E, Che J, Heirich K, et al. Profiling protein expression in circulating tumour cells using microfluidic western blotting. Nat Commun. 2017;8(14622). [PubMed: 28364116]

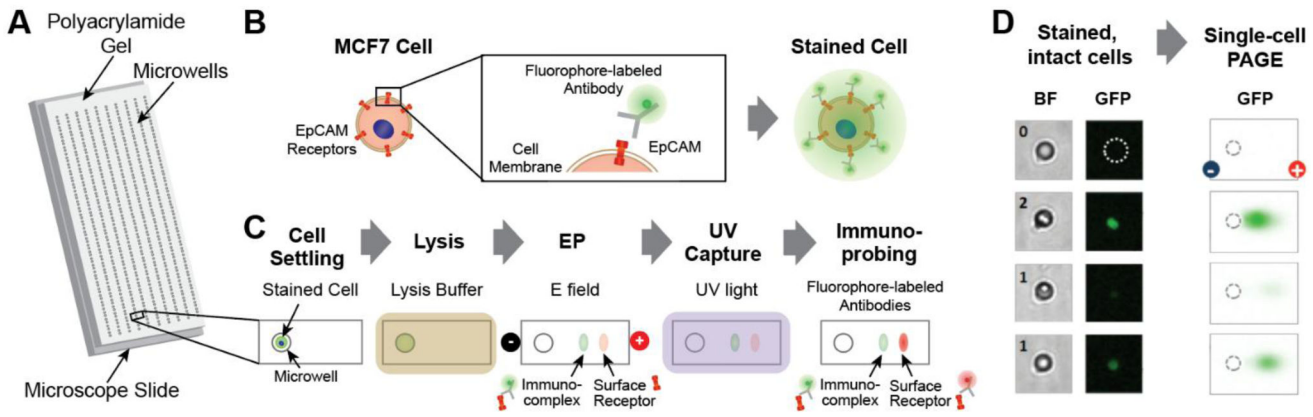

Figure 1.

Concurrent detection of surface EpCAM immunocomplex and intracellular EpCAM using mobility shift single-cell electrophoresis. (A) Brightfield image of the single-cell PAGE device, showing a thin PA gel layer grafted on a microscope slide and stippled with an array of microwells. (B) Schematic of EpCAM receptors on surface of MCF7 cells stained with fluorophore-labeled anti-EpCAM antibodies. (C) Integration of live-cell immunofluorescence with the single-cell PAGE assay. Unfixed cells stained with fluorescently conjugated antibodies are settled into microwells for subsequent lysis, protein PAGE, and photo-blotting of separated proteins. Unstained targets can be immunoprobed with additional fluorophore-conjugated antibodies. (D) Bright field (BF) and fluorescence (GFP) micrographs of MCF7 cells stained with anti-EpCAM* and seated in microwells. False-colored fluorescence micrographs show surface EpCAM immunocomplex fluorescence blots after migration into the PA gel.

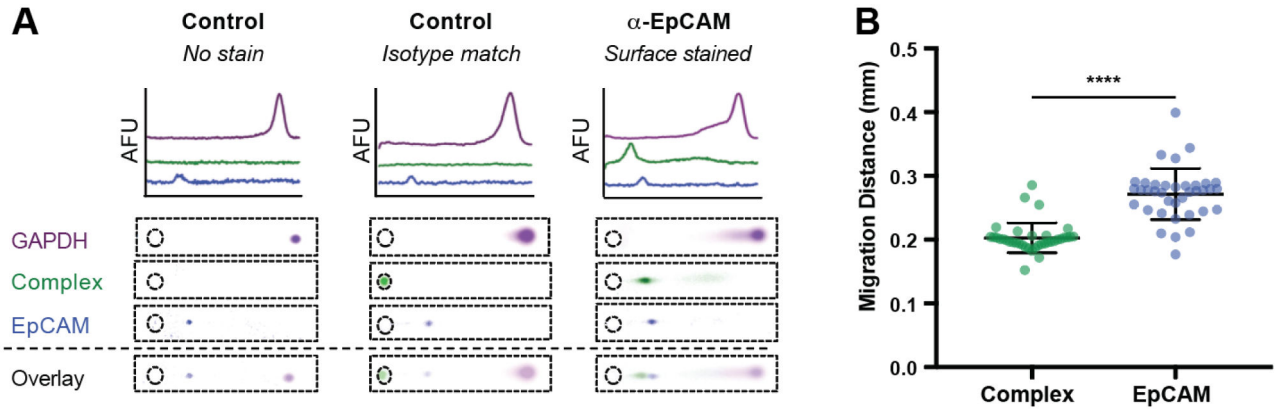

Figure 2.

Single-cell PAGE detects an electrophoretic mobility shift of the surface EpCAM immunocomplex, as compared to free EpCAM. (A) Stained, unstained, and isotype matched stained MCF7s were assayed by single-cell PAGE (Lysis buffer: 0.5% SDS, 0.1% Triton X-100, 0.25%, Na-DOC, 50oC, lysis for 20 s and electrophoresis for 25 s). Fluorescence intensity profiles for false-colored fluorescence micrographs of GAPDH, antibody-EpCAM immunocomplex and EpCAM are shown for the three conditions. (B) Violin plots of migration distance of the immunocomplex and free EpCAM demonstrates a reduction in electrophoretic mobility of the surface EpCAM immunocomplex with respect to the free EpCAM (Mann Whitney U test, p value < 0.0001, N = 37).

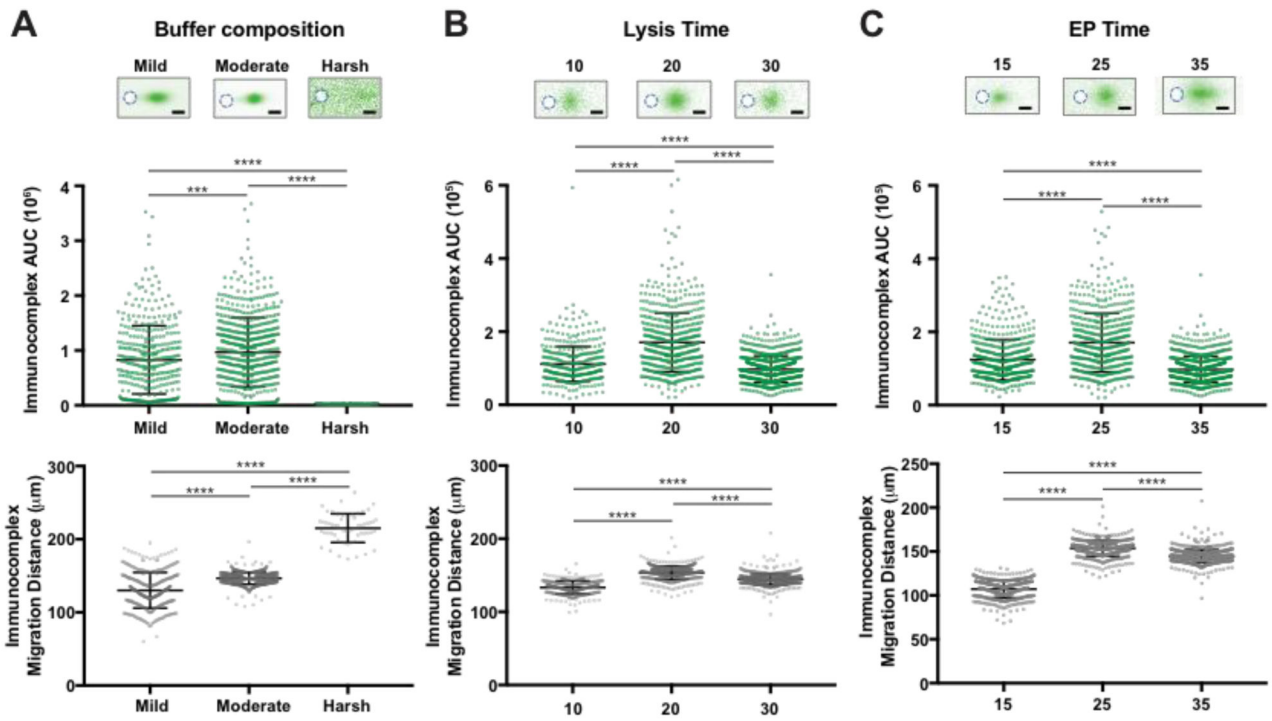

Figure 3.

Cell lysis conditions determine compatibility between surface antibody immunofluorescence and single-cell PAGE. The effects of (A) buffer composition, (B) lysis time (tlysis) and (C) electrophoresis time (tEP) on immunocomplex AUC and migration distance are displayed in the corresponding false-colored fluorescence micrographs (top) and violin plots (bottom) for each condition. Mann Whitney U tests, where '***' and '****' represent p values of <0.001 and < 0.0001. (a) N = 387, 670 and 59 cells for mild, moderate and harsh, respectively. (b) N = 364, 567 and 854 cells for tlysis = 10, 20 and 30 s, respectively. (c) N = 539, 567 and 854 cells for tEP = 15, 25 and 35 s, respectively.

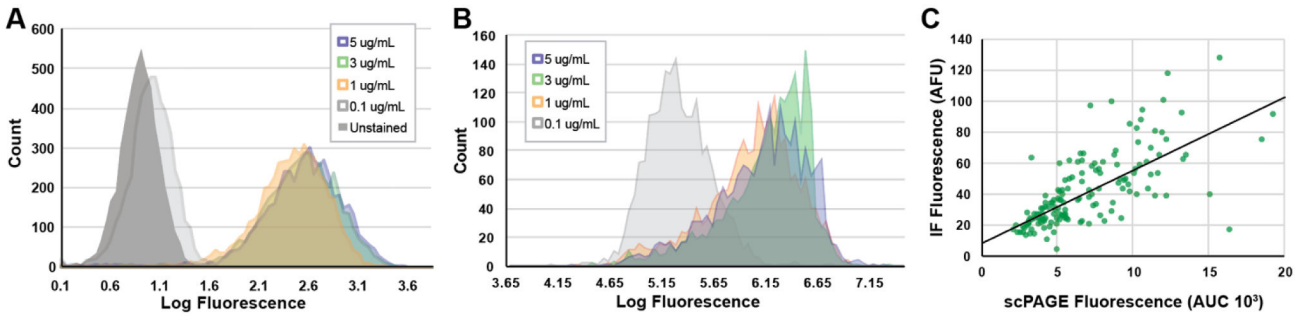

Figure 4.

Validation of single-cell PAGE with gold standard single-cell surface receptor measurements. Histograms of fluorescence intensity (Log Fluorescence) for MCF7 cells stained with anti-EpCAM* measured by (A) flow cytometry and (B) single-cell PAGE result in high distribution overlaps for antibody concentrations of 1.0. 3.0 and 5.0 μg/mL, but not 0.1g/mL. (C) Bivariate plot of fluorescence for anti-EpCAM* stained MCF7 cells measured by immunofluorescence (IF) prior to lysis and single-cell PAGE after lysis and electrophoresis, showing a strong, linear correlation between fluorescence intensity measured by IF and single-cell PAGE (Pearson correlation, = 0.694, p value < 0.00001, N = 148 microwells containing single cells).